THE ASTROPHYSICAL JOURNAL, 451:616–623, 1995 October 1

DISCOVERY OF HIGHLY IONIZED HIGH-VELOCITY CLOUDS TOWARD MARKARIAN 509[1]

KENNETH R. SEMBACH,[2,3] BLAIR D. SAVAGE,[4] LIMIN LU,[2,5] AND EDWARD M. MURPHY[6]

Received 1994 December 13; accepted 1995 April 11

ABSTRACT

We present Goddard High Resolution Spectrograph measurements of the Milky Way halo gas absorption toward Mrk 509 ($l = 36.^\circ0$, $b = -29.^\circ9$) in the 1233–1268 and 1521–1558 Å spectral regions at a resolution of ≈ 15 km s^{-1}. We detect high-velocity ($v_{LSR} \approx -340$ to -170 km s^{-1}) absorption in both members of the C IV $\lambda\lambda$1548, 1550 doublet but find no corresponding Si II λ1526 or N V λ1238 absorption. The high-velocity C IV absorption has substructure that can be modeled with two Gaussian components centered at $\langle v_{LSR} \rangle = -227.5 \pm 6.1$ and -283.4 ± 3.2 km s^{-1} with N(C IV)/N(Si II) > 1.3 and 5.1 and N(C IV)/N(N V) > 3.0 and 6.6, respectively. To understand the relationship between these highly ionized C IV high-velocity clouds (HVCs) and the more familiar H I HVCs, we obtained sensitive observations of the H I 21 cm emission toward Mrk 509 with the NRAO 140 foot (43 m) telescope. We find no detectable 21 cm emission at the velocities of the C IV HVCs to a 4 σ limit of N(H I) < 4.9×10^{17} cm^{-2}, but mapping of the 21 cm emission in the area around Mrk 509 indicates that H I HVCs with $\langle v_{LSR} \rangle$ between -270 and -300 km s^{-1} are located within approximately $1.^\circ5$ of the sight line. This suggests that the C IV HVC absorption probes the ionized boundaries of the H I HVCs. Although we cannot completely rule out collisional ionization at $T \geq 10^5$ K as a means for producing some of the high-velocity C IV, the observed ionic ratios are sufficiently rigorous for us to reject many collisional ionization models and favor a photoionization interpretation of the ionization structure of the C IV HVCs. A plane-parallel slab model investigated using the photoionization code CLOUDY suggests that the high-velocity C IV absorption can be explained with an almost fully ionized [N(H I)/N(H$_{tot}$) < 0.01] subsolar metallicity layer (≥ 1 kpc) of low-density gas ($\leq 10^{-2}$ cm^{-3}) photoionized by an extragalactic ionizing background with J_ν(Lyman-limit) $\sim 10^{-22}$ ergs cm^{-2} s^{-1} Hz^{-1} sr^{-1}. The general properties of the high-velocity C IV absorption more closely resemble those of the high-ionization quasar metal line absorption systems than those of other sight lines through the Milky Way disk and halo.

Subject headings: galaxies: individual (Markarian 509) — Galaxy: halo — ISM: abundances — ISM: clouds — radio lines: ISM — ultraviolet: ISM

1. INTRODUCTION

One of the fundamental obstacles to overcome in understanding the nature of the Milky Way halo is being able to detect absorption by gas at large distances from the Galactic plane that is uncontaminated by absorption arising in disk gas. This leads to the somewhat ironic dilemma that, although evidence continues to favor very large (>40 kpc) halos of distant intervening galaxies as the source of the narrow absorption metal line systems (Bergeron & Boisse 1991; Steidel 1993), the extent and properties of a similar halo have yet to be determined for the Milky Way. Observations of H I high-velocity clouds (HVCs) in the Galaxy may represent our best hope for studying the properties of distant halo gas as they cover about 37% of the sky at 21 cm wavelengths (Murphy, Lockman, & Savage 1995), seem to be situated at large distances from the Galactic plane (de Boer et al. 1994), and, by definition, are distinct from lower velocity gas clouds located primarily in the Galactic disk.

It has become possible to effectively probe the Milky Way halo toward QSOs and bright galactic nuclei with the ultraviolet spectrographs aboard the *Hubble Space Telescope* (*HST*) (see Lu, Savage, & Sembach 1994a, b; Sembach, Savage, & Lu 1995; Savage, Sembach, & Lu 1995, hereafter Papers I–IV, respectively). This is especially important because now the properties of high-velocity gas along many sight lines through the halo can be explored through diagnostic line information available in the ultraviolet regions of the spectrum. Ultraviolet studies of the interstellar absorption toward bright stars in the Magellanic Clouds before *HST* (Savage & de Boer 1981; Fitzpatrick & Savage 1983; Savage et al. 1989) indicated that the neutral and weakly ionized disk and halo gas toward the Clouds is many times more abundant than its highly ionized counterpart and, until recently, have served as the primary benchmarks for comparisons between the ionization properties of the Milky Way and quasar absorption systems (Wolfe 1983; Hartquist & Dyson 1984).

In this article we present Goddard High Resolution Spectrograph (GHRS) measurements of high-velocity ($v_{LSR} \approx -340$ to -170 km s^{-1}) C IV absorption in the Milky Way halo toward the Seyfert galaxy Mrk 509. We find the high-velocity absorption to be typical of the high-ionization metal line systems toward quasars in that, even though C IV is strong, there is no detectable low-ion (Si II) absorption. In § 2 we discuss these observations and present new NRAO 21 cm measurements of

[1] Based on observations obtained with the NASA/ESA *Hubble Space Telescope*, obtained at the Space Telescope Science Institute, which is operated by the Association of Universities for Research in Astronomy, Inc., under NASA contract NAS5-26555.

[2] Hubble Fellow.

[3] Center for Space Research, Massachusetts Institute of Technology, Cambridge, MA 02139.

[4] Washburn Observatory, University of Wisconsin–Madison, Madison, WI 53706.

[5] Department of Astronomy, 105-24, California Institute of Technology, Pasadena, CA 91125.

[6] National Radio Astronomy Observatory, Charlottesville, VA 22903.

high-velocity H I gas in the general direction of Mrk 509. We present our analysis of the data in § 3, and in § 4 we discuss the relationship between the high-velocity C IV absorption and H I emission in the direction of Mrk 509, the ionization properties of the C IV clouds, and the implications of these observations for understanding the origins of quasar absorption lines and the extended halos of the Milky Way and other galaxies. In a future paper we will examine the low-velocity absorption from the Milky Way disk and halo.

2. OBSERVATIONS AND MEASUREMENTS

2.1. *HST Data*

We obtained GHRS intermediate-resolution (G160M) observations of the 1233–1268 and 1521–1558 Å spectral regions of Mrk 509 during 1993 May and 1994 August as part of GO programs 3463 and 5300, which were designed to study halo gas at large distances from the Sun. For both observations, the light of Mrk 509 entered the large (2".0 × 2".0) science aperture. We used standard carousel rotation (FP-Split = 4) and spectrum deflection (Comb-Addition = 4) procedures to reduce fixed pattern noise structure in each spectrum caused by irregularities in the detector window and photocathode response. We also used a substep pattern (Step-Patt = 4) to provide full diode array observations of the off-spectrum backgrounds, which we averaged and subtracted from the on-spectrum data. The on-spectrum exposure times were 3072 and 3584 s in the 1250 and 1544 Å spectral regions, respectively. Each spectrum had a sampling interval of 2 substeps per diode to satisfy the Nyquist sampling requirement across the 1 diode resolution element. The *HST* archive identifications of the science data are Z1790208M and Z26O0108T.

The 1250 Å observation was obtained prior to the *HST* corrective optics installation and suffers from a degraded resolution. The pre-COSTAR instrumental spread function for this large science aperture observation consists of a narrow (FWHM $\approx$ 20 km s^{-1}) core containing approximately 40% of the spread-function area and broad ($\approx \pm$ 70 km s^{-1}) wings containing approximately 60% of the area. The 1540 Å large science aperture observation obtained after the servicing mission has a nearly Gaussian instrumental profile and a velocity resolution of approximately 14 km s^{-1} (FWHM). For more information about the GHRS and its performance see Duncan (1992).

For the 1540 Å observation we obtained a Pt-lamp wavelength calibration at the same grating carousel position as the science data to reduce the ± 1 diode uncertainty in the standard GHRS heliocentric wavelength determination to approximately 0.2 diode ($\approx$3 km s^{-1}). Since the wavelength calibration depends on the position of the object in the large science aperture, we also obtained an image field map of the aperture prior to the science observation to be certain that Mrk 509 was centered by the acquisition and peak-up procedures. We then registered the 1250 Å observation to the longer wavelength spectrum by aligning the absorption produced by the interstellar Si II λ1260 and Si II λ1526 absorption lines. We applied a local standard of rest (LSR) correction of $v_{\rm LSR} = v_{\rm helio} + 8.9$ km s^{-1} to all heliocentric velocities.

In Figure 1 we plot continuum-normalized profiles of the Si II λ1526, C IV $\lambda\lambda$1548, 1550, and N V λ1238 lines detected in the GHRS spectra of Mrk 509. We determined the local continua for the lines by fitting low-order polynomials to regions near each absorption feature (see Sembach & Savage 1992).

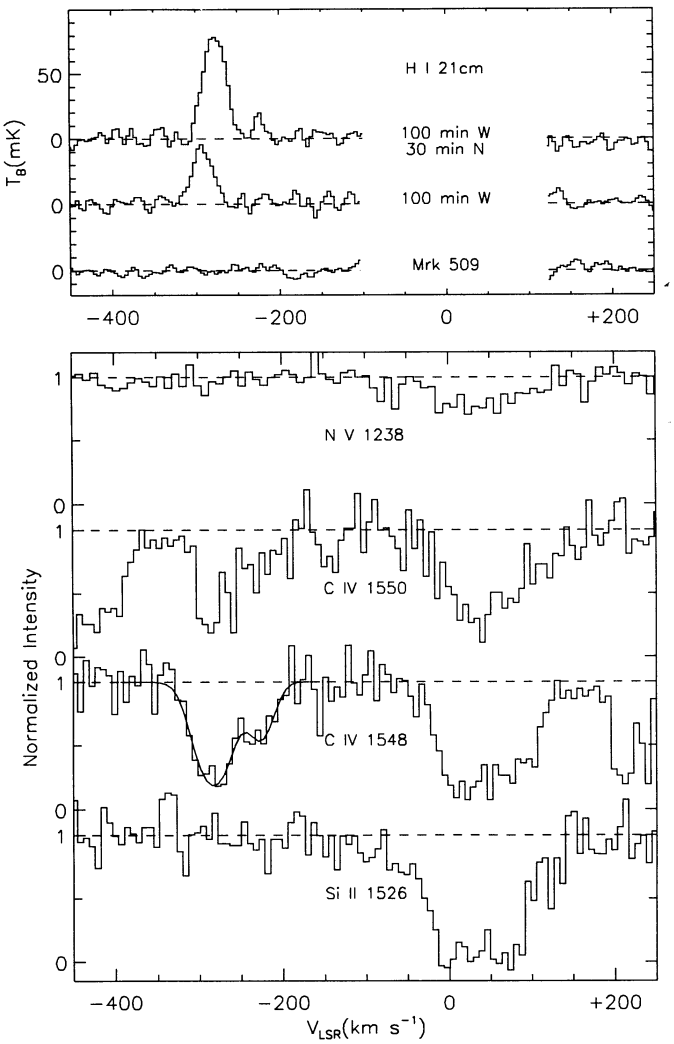

FIG. 1.—*Top*: Brightness temperature vs. LSR velocity for the H I 21 cm emission measured in the direction of Mrk 509 and at two nearby positions where high-velocity H I is seen. These NRAO 140 foot telescope spectra have a velocity resolution of $\approx$8 km s^{-1} and an angular resolution of 21′. The 21 cm emission measurement toward Mrk 509 has an rms baseline fluctuation level of 2.1 mK and a 4 σ H I detection threshold of 4.9 × 10^{17} cm^{-2} (see Table 2). *Bottom*: Continuum-normalized intensity vs. LSR velocity for the Si II λ1526, C IV $\lambda\lambda$1548, 1550, and N V λ1238 lines in our GHRS G160M spectra of Mrk 509. The Si II and C IV spectra have S/N $\approx$ 7 and a resolution of $\approx$14 km s^{-1} (FWHM). The N V measurements were obtained before the corrective optics were installed on *HST* and therefore have a somewhat lower resolution than the post-COSTAR data shown (see text). Note the presence of the strong C IV HVCs between −340 and −170 km s^{-1}. A two-component fit to the high-velocity C IV absorption is overplotted on the λ1548 spectrum (*thin solid line*).

Absorption produced in the disk and low halo environments of the Milky Way at $-75 \le v_{\rm LSR} \le +150$ km s^{-1} is readily visible in all three species, as is high-velocity C IV absorption between −340 and −170 km s^{-1}. In Table 1 we list the rest wavelengths, oscillator strengths, and high-velocity gas equivalent widths of the Si II, S II, C IV, and N V lines. The errors on W_λ in Table 1 are ± 1 σ uncertainties due to continuum placement errors and statistical noise fluctuations in the data.

We do not list high-velocity gas equivalent widths of the Si II λ1260 or S II λ1259 lines in Table 1, even though the short-wavelength G160M observation covers these lines. The S II λ1259 line spans the Si II λ1260 velocity range from −300 to

TABLE 1

HVC Equivalent Widths and Column Densities

Line[a]	f[a]	$v_{LSR} = -340$ to -250 km s^{-1} W_λ (mÅ)	log N	$v_{LSR} = -250$ to -170 km s^{-1} W_λ (mÅ)	log N
H I 21 cm[b]	...	...	<17.69	...	<17.69
Si II λ1526.707[c]	0.1155	-5 ± 23	<13.29	11 ± 20	<13.33
S II λ1250.584[c]	0.0054	2 ± 6	<14.27	0 ± 5	<14.12
λ1253.811[c]	0.0109	3 ± 5	<13.93	0 ± 5	<13.82
C IV λ1548.195[d]	0.1908	218 ± 17	>14.00	89 ± 17	>13.46
λ1550.770[d]	0.0952	186 ± 17	>14.19	70 ± 18	>13.65
N V λ1238.821[c]	0.1570	10 ± 11	<13.18	3 ± 9	<12.98

[a] Wavelengths and f-values from the data compilation prepared by Morton 1991, except for f_{1526}, which is from Dufton et al. 1983. The listed value appears to be in better agreement with the measured Si II line strengths toward HD 93521 (Spitzer & Fitzpatrick 1993) than the value listed by Morton.

[b] H I upper limits (4 σ) derived for an rms noise fluctuation level of 2.1 mK and a Gaussian velocity distribution with FWHM = 30 km s^{-1}.

[c] Si II, S II, and N V upper limits (2 σ) derived from integration of the apparent column density profiles produced by application of eq. (2) to the normalized profiles shown in Fig. 1. The results are consistent with those from a linear curve of growth applied to the listed values of W_λ.

[d] C IV lower limits derived from integration of the apparent column density profiles produced by application of eq. (2) to the normalized profiles shown in Fig. 1. A two-component fit to the high-velocity portions of the C IV λ1548 profile yields similar results. Throughout our discussion of the data, we adopt the more conservative values of log N(C IV) > 14.00 and 13.46 found for the λ1548 line, due to the noisier character of the λ1550 line.

-130 km s^{-1}, and an intergalactic H I line spans the S II λ1259 velocity range from -650 to -170 km s^{-1}. We must therefore rely on the Si II λ1526 and S II λλ1250, 1253 lines in our analysis of the HVC absorption.

No previous observations of Mrk 509 with the *IUE* satellite (York et al. 1982, 1984) or ground-based observatories (Blades & Morton 1983; Morton & Blades 1986) have revealed absorption by neutral or ionized species in the $-340 \leq v_{LSR} \leq +170$ km s^{-1} range of the high-velocity C IV. As we shall see in § 4, this high-velocity C IV absorption is probably related to several H I clouds located in the Galactic halo in this area of the sky. It is unlikely that the C IV absorption is associated with Mrk 509 due to the very high ejection velocity required [approximately $+10^4$ km s^{-1} for z(Mrk 509) = 0.0345; Phillips et al. 1983] and the lack of detectable N V at similar velocities (see Foltz et al. 1988).

2.2. *NRAO Data*

To complement the *HST* data, we also obtained H I 21 cm emission spectra for the Mrk 509 sight line and 22 nearby positions using the NRAO 140 foot (43 m) telescope. In Figure 1 we show the 21 cm spectrum for Mrk 509 and two nearby positions where H I is detected (100′ west of Mrk 509 and 100′ west, 30′ north of Mrk 509). The data have an angular resolution of 21′ and a velocity resolution of 8 km s^{-1} after Hanning smoothing. We used a second-order polynomial to determine the baseline for each spectrum. Only data for $|v_{LSR}| > 100$ km s^{-1} is shown for the H I data in Figure 1 because the emission at lower velocities is not completely removed from the spectrum by the ±1°.7 position switching (on-off source) used to detect the weak, high-velocity features. Further details about the observational techniques and data reduction are given by Murphy et al. (1995).

From the 21 cm emission spectrum for Mrk 509 shown in Figure 1, we estimate a 4 σ upper limit of log N(H I) < 5×10^{17} cm^{-3} derived from the baseline rms of 2.1 mK and the following equation:

$$N(\text{H I}) = 1.942 \times 10^{18} \Delta v T_{max} \text{ atoms cm}^{-2}, \quad (1)$$

where Δv is the FWHM of the best-fit Gaussian profile in km s^{-1} (assumed to be 30 km s^{-1} for cases when no line is detected), T_{max} is the peak brightness temperature of the line in kelvins (assumed to be 4 times the baseline rms when no line is detected), and the H I is assumed to be optically thin. Table 2 contains values of T_{max}, Δv, $\langle v_{LSR} \rangle$, and log N(H I) for NRAO 21 cm measurements at 22 positions within ≈2° of Mrk 509. We detect H I emission near -280 km s^{-1} in only six cases, all at locations north or west of Mrk 509. There is no detectable high-velocity H I emission immediately south or east of Mrk 509.

In Figure 2 we provide a map of the H I sky in the direction of Mrk 509 in Galactic coordinates. Filled circles represent those cases where we have detected high-velocity 21 cm emission, and plus signs denote nondetections. Our H I pointings were made at 10′ spacings on an east-west line and were chosen to map the edge of the HVC. To improve the spectral baselines, we position-switched the telescope against a reference position which was ≈1°.7 east of the target position. In Figure 2, the target positions are above Mrk 509 and the reference positions are below Mrk 509. Open circles in Figure 2 indicate the H I HVCs detected by Hulsbosch & Wakker (1988) down to a detection level of $\approx 2 \times 10^{18}$ cm^{-2}. The average velocities of the Hulsbosch & Wakker clouds are indicated within the circles. Most of these H I HVCs occur at longitudes $l > 36°$. The symbol sizes in Figure 2 reflect the true FWHM beam sizes of the telescopes used for the observations.

3. ANALYSIS

The high-velocity C IV absorption toward Mrk 509 contains substructure having a strong component between -340 and -250 km s^{-1} and a weaker component between -250 and

TABLE 2

NRAO 21 cm Line Profile Results and H I Column Densities

l	b	North[a]	East[a]	T_{max}[b] (mK)	FWHM (km s^{-1})	$\langle v_{LSR} \rangle$ (km s^{-1})	N(H I)[c] (cm^{-2})
36°.00	−29°.90.....	(Mrk 509)		<2.1	...	...	$<4.9 \times 10^{17}$
35.17	−28.38.....	0′	−100′	39.3 ± 3.1	28.1 ± 4.3	−292.7 ± 1.8	$(2.1 \pm 0.4) \times 10^{18}$
35.25	−28.53.....	0	−90	22.8 ± 1.9	28.2 ± 2.8	−296.8 ± 1.2	$(1.2 \pm 0.2) \times 10^{18}$
35.33	−28.68.....	0	−80	<2.8	...	...	$<6.5 \times 10^{17}$
36.08	−30.05.....	0	+10	<4.9	...	...	$<1.1 \times 10^{18}$
36.17	−30.20.....	0	+20	<2.8	...	...	$<6.5 \times 10^{17}$
36.85	−31.42.....	0	+100	<2.1	...	...	$<4.9 \times 10^{17}$
35.59	−28.57.....	+15	−80	23.0 ± 0.3	23.0 ± 3.0	−275.6 ± 1.2	$(1.0 \pm 0.1) \times 10^{18}$
35.67	−28.72.....	+15	−70	<3.4	...	...	$<7.9 \times 10^{17}$
36.43	−30.09.....	+15	+20	<3.8	...	...	$<8.2 \times 10^{17}$
36.51	−30.24.....	+15	+30	<3.4	...	...	$<7.9 \times 10^{17}$
35.68	−28.16.....	+30	−100	67.5 ± 0.8	30.7 ± 0.5	−277.7 ± 0.2	$(4.0 \pm 0.1) \times 10^{18}$
35.85	−28.46.....	+30	−80	22.7 ± 1.4	24.9 ± 1.8	−275.2 ± 0.7	$(1.1 \pm 0.1) \times 10^{18}$
35.93	−28.61.....	+30	−70	12.1 ± 1.1	24.5 ± 2.7	−276.4 ± 1.1	$(5.8 \pm 0.8) \times 10^{17}$
36.01	−28.76.....	+30	−60	<4.4	...	...	$<1.0 \times 10^{18}$
36.52	−29.68.....	+30	0	<2.9	...	...	$<6.8 \times 10^{17}$
36.69	−29.98.....	+30	+20	<5.0	...	...	$<1.2 \times 10^{18}$
36.77	−30.13.....	+30	+30	<2.9	...	...	$<6.8 \times 10^{17}$
36.85	−30.29.....	+30	+40	<4.4	...	...	$<1.0 \times 10^{18}$
34.50	−28.29.....	−30	−120	<6.5	...	...	$<1.5 \times 10^{18}$
34.66	−28.59.....	−30	−100	<4.5	...	...	$<1.0 \times 10^{18}$
35.32	−29.81.....	−30	−20	<6.5	...	...	$<1.5 \times 10^{18}$
35.48	−30.11.....	−30	0	<4.5	...	...	$<1.0 \times 10^{18}$

[a] North and east refer to the beam position relative to Mrk 509 in equatorial coordinates (units are arcminutes). Negative numbers indicate positions south and west of Mrk 509.

[b] Upper limits denote rms baseline fluctuations. The maximum temperature is likely to be less than 4 times the listed value.

[c] H I column density and 1 σ errors derived from the NRAO 21 cm emission line measurements using eq. (1). Upper limits are 4 σ estimates assuming FWHM = 30 km s^{-1}.

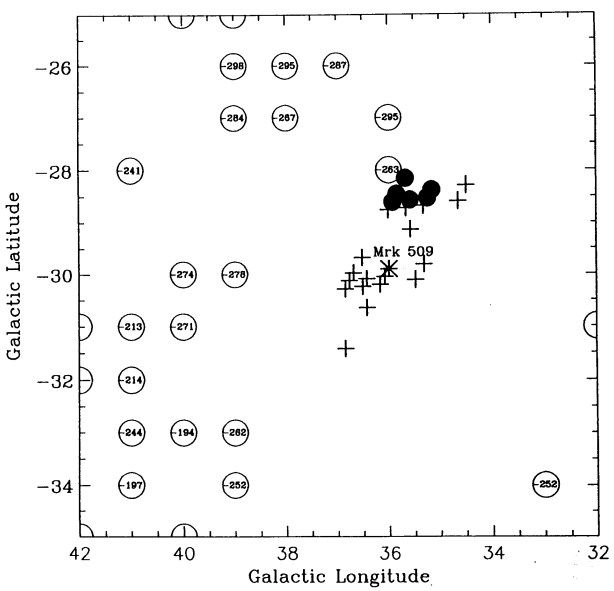

Fig. 2.—Map in Galactic coordinates of the area surrounding Mrk 509 showing the distribution of H I 21 cm HVCs. Open circles are detections of H I HVCs from the catalog of Hulsbosch & Wakker (1988), which is complete to a column density detection limit of 2×10^{18} cm^{-2}. The velocities of the clouds are shown inside the circles. Note that the entire region shown in the figure has been searched for H I HVCs by Hulsbosch & Wakker with a 1° × 1° grid, so empty regions represent areas where no HVCs with N(H I) > 2×10^{18} cm^{-2} were detected in their survey. Filled circles (detections) and plus signs (nondetections) mark the positions where we have conducted more sensitive searches in 21 cm (see Table 2). The symbol sizes reflect the true FWHM beam sizes of the telescopes used for the observations.

−170 km s^{-1}. The most direct approach to estimating the C IV column density in each interval is to convert the normalized absorption profiles shown in Figure 1 into measures of apparent column density per unit velocity and integrate each line over the appropriate velocity range:

$$N_a = \int N_a(v)\,dv = \int \frac{m_e c/\pi e^2}{f\lambda(\text{Å})}\,\tau_a(v)\,dv$$

$$= \frac{3.768 \times 10^{14}}{f\lambda(\text{Å})} \int \ln\frac{1}{I(v)}\,dv \text{ atoms cm}^{-2}\,(\text{km s}^{-1})^{-1}\,. \quad (2)$$

Here, $\tau_a(v)$ is the apparent (observed) optical depth for the measured intensity at velocity v, and f is the oscillator strength of the transition. Equation (2) yields

$$\log N_a(\text{C IV})_{1548} = 14.00^{+0.04}_{-0.04}\,,$$

$$\log N_a(\text{C IV})_{1550} = 14.19^{+0.04}_{-0.04}\,,$$

for the −283 km s^{-1} component, and

$$\log N_a(\text{C IV})_{1548} = 13.46^{+0.08}_{-0.09}\,,$$

$$\log N_a(\text{C IV})_{1550} = 13.65^{+0.10}_{-0.12}\,,$$

for the −228 km s^{-1} component. The weaker member of the doublet yields higher values of log N_a for both velocity intervals, which implies that some unresolved saturated structure may exist within the C IV profiles [i.e., N(C IV) ≥ N_a(C IV); see Savage & Sembach 1991]. Given the likelihood that much of the high-velocity C IV along the Mrk 509 sight line arises in warm photoionized gas (see § 4.2), any narrow components

within the profiles are probably not strong enough to require large saturation corrections to the column densities of the integrated profiles as the thermal width of a C IV line produced in 8000 K gas is 5.5 km s^{-1} (FWHM), or only 2–3 times less than the instrumental width. The inherently low S/N (≈ 7) of the data makes the modest saturation corrections implied by the above estimates of log N_a unreliable, so we adopt the conservative approach of assigning lower limits of log N(C IV) > 14.00 and 13.46 for the two velocity ranges based on the λ1548 line results.

We have fitted two Gaussian components to the C IV data between -400 and -100 km s^{-1} to further quantify the character of the absorption for later discussions. Our ability to reliably describe the velocity distribution with only two components is limited by the S/N of the data. For this reason, we fit only the stronger λ1548 line to reduce the complications caused by including the weaker λ1550 line and attempting to fit the lines simultaneously. We find

$$\log N(\text{C IV}) = 14.00^{+0.06}_{-0.06}, \quad b = 25.2 \pm 2.2 \text{ km s}^{-1},$$
$$\langle v_{\text{LSR}} \rangle = -283.4 \pm 3.2 \text{ km s}^{-1},$$

and

$$\log N(\text{C IV}) = 13.45^{+0.24}_{-0.20}, \quad b = 18.7 \pm 5.6 \text{ km s}^{-1},$$
$$\langle v_{\text{LSR}} \rangle = -227.5 \pm 6.1 \text{ km s}^{-1}.$$

These column densities are the same as those found for the λ1548 line by the direct integration method. A discussion of the fitting algorithm and minimization process has been given by Sembach, Danks, & Savage (1993). We plot the best-fit profile on top of the C IV λ1548 data in Figure 1.

Equation (2) can also be used to provide upper limits on the Si II and N V column densities for the lines shown in Figure 1. Table 1 contains a summary of the 2 σ upper limits on the column density derived for each line by direct integration of the profiles over the $-340 \le v_{\text{LSR}} \le -250$ km s^{-1} and $-250 \le v_{\text{LSR}} \le -170$ km s^{-1} velocity ranges. For completeness, we also list the column density limits derived for the S II $\lambda\lambda$1250, 1253 lines in the 1250 Å spectrum, although the S II limits do not place strong constraints on the properties of the high-velocity gas. The upper limits for Si II, S II, and N V are consistent with those found from application of a linear curve of growth to the listed values of W_λ. Sembach & Savage (1992) provide a discussion of the derivation of the errors associated with the direct integration of apparent column density profiles (see their Appendix A). Combining the column densities of Si II, C IV, and N V yields the following ionic ratios:

$$N(\text{C IV})/N(\text{Si II}) > 5.1, \quad N(\text{C IV})/N(\text{N V}) > 6.6,$$

for the -283 km s^{-1} component, and

$$N(\text{C IV})/N(\text{Si II}) > 1.3, \quad N(\text{C IV})/N(\text{N V}) > 3.0,$$

for the -228 km s^{-1} component. These results are summarized in Table 3 together with the ratios of C IV to Si II and C IV to N V found for the high-velocity gas along three extragalactic sight lines (NGC 3783, H1821+643, and Fairall 9) and one extended Galactic sight line (HD 156359) studied in previous papers in this series.

TABLE 3

SIGHT LINE COMPARISON

Paper and Object	(l, b)	v_{LSR} (km s^{-1})	$\frac{N(\text{C IV})^a}{N(\text{Si II})}$	$\frac{N(\text{C IV})^a}{N(\text{N V})}$
I. NGC 3783	(287°, +23°)	+240	<0.65	...
II. HD 156359[b]	(329, −14)	+125	<3.3	<3.4
III. Fairall 9	(295, −59)	+170	<0.15	...
		+210	<0.14	...
IV. H1821+643	(94, +27)	−125	<0.35	>1.5
		−215[c]	>0.9	>0.4
V. Mrk 509	(36, −30)	−228	>1.3	>3.0
		−283	>5.1	>6.6

[a] Two sigma limit.

[b] HD 156359 is a halo star in the inner Galaxy at $d = 11.1$ kpc and $z = -2.8$ kpc.

[c] Possible C IV HVC of the type found toward Mrk 509.

4. DISCUSSION

The C IV HVCs we have detected in the direction of Mrk 509 are distinct in their ionization properties from classic H I HVCs and may provide a unique chance to explore the processes occurring in the boundaries of the high-velocity H I clouds. It is therefore important to understand the relationship of these two types of HVCs and to identify their common properties.

4.1. H I *Sky in the Direction of Mrk 509*

Several HVCs detected in sensitive H I 21 cm emission surveys exist in the general direction of Mrk 509. These clouds typically consist of several components with LSR velocities between -300 and -200 km s^{-1} and belong to a complex of H I HVCs known as the Galactic center negative velocity (GCN) clouds (Wakker & van Woerden 1991).[7] The locations of some of these clouds are shown in Figure 2. The origin of the GCN complex is still a subject of discussion, but the large peculiar velocities of the clouds argue strongly against a quiescent origin within the Galactic halo. In the direction of Mrk 509, gas following the Galactic rotation curve derived by Clemens (1985) has $0 \le v_{\text{LSR}} \le +80$ km s^{-1} for $d \le 16$ kpc and a limiting velocity of ≈ -112 km s^{-1} at larger distances, assuming the gas rotational velocity is independent of distance from the Galactic plane. Though intergalactic H I clouds or low surface brightness galaxies are possible explanations for some of the GCN emission at 21 cm (Cohen & Mirabel 1978; Mirabel & Cohen 1979), the GCN complex is more likely associated with an extension of the Magellanic Stream (MS) in which gas is flowing in toward the disk near the Galactic center (Mirabel 1981, 1982; Giovanelli 1981; Wakker & van Woerden 1991). Recent modeling of the MS by Moore & Davis (1994) indicates that the motions of many of these clouds can be explained if they are the debris from previous passages of the LMC through the thick disk of the Milky Way. Both the H I HVCs and C IV HVCs in this direction are almost surely under the gravitational influence of the Milky Way since their negative velocities indicate that they are moving toward the Galactic plane.

To investigate the extent of high-velocity H I in the direction of Mrk 509 we obtained 21 cm spectra at the locations indicated in Figure 2 (see § 2). The spectra illustrated in Figure 1 for two positive detections near to the Mrk 509 sight line show that the emission is confined primarily to a single component with a central velocity similar to that of the -283 km s^{-1} C IV component ($\langle v_{\text{LSR}} \rangle = -292.0 \pm 0.7$ km s^{-1} at 100′ west;

[7] Some GCN clouds near the Mrk 509 sight line in their catalog include Nos. 419, 442, 443, 445, 453, 461, 482, and 489.

$\langle v_{LSR} \rangle = -276.9 \pm 0.6$ km s^{-1} at 100′ west, 30′ north). The widths of the H I emission profiles are similar to the 19–25 km s^{-1} widths of the high-velocity C IV absorption components, and in both cases turbulent motions in the gas may account for most of the line broadening since thermal broadening alone would imply relatively large temperatures for each species ($T \approx 2.4$–4.6×10^5 K for C IV and $T \approx 1.5$–2.0×10^4 K for H I). Given the velocity similarities between the C IV HVC absorption and the nearby high-velocity H I emission, it seems reasonable to conclude that the C IV HVCs trace the outer ionized region(s) of one or more of the H I HVCs.

We can make a very rough estimate of the covering fraction of the C IV HVCs in the Galaxy for comparison with the H I HVC results. In Paper IV we found a weak C IV HVC toward H1821+643 ($l = 94°$, $b = 127°$) at -215 km s^{-1} that has ionization properties consistent with those of the C IV HVCs toward Mrk 509 but a strength about 10 times smaller. Intermediate-resolution GHRS observations of Milky Way halo gas along the other sight lines in this series of papers (Table 3) and toward Mrk 205 (Bowen & Blades 1993) and 3C 273 (Savage et al. 1993b) have not revealed any C IV HVCs of the type found in this study. However, Bruhweiler et al. (1993) have reported the possible detection of a Galactic C IV HVC at ≈ -260 km s^{-1} toward PKS 2155−304 ($l = 17°$, $b = -52°$) based on a low-resolution (FWHM ≈ 150 km s^{-1}) GHRS spectrum. Unfortunately, the N V line toward PKS 2155−304 is severely contaminated by intergalactic H I which makes an estimate of N(C IV)/N(N V) in the high-velocity gas impossible.

From the information available for this small number of sight lines, it appears that the covering fraction of the C IV HVCs is ~38% (three out of eight sight lines). Additional observations of other extragalactic background sources at intermediate resolutions with the GHRS and future Space Telescope Imaging Spectrograph are needed to more precisely quantify the C IV HVC covering fraction. It is interesting that this rough estimate is approximately the same as the covering fractions found for H I HVCs through sensitive 21 cm observations [37% for N(H I) $\geq 7 \times 10^{17}$ cm^{-2}; Murphy et al. 1995] and ultraviolet absorption by strong resonance lines of singly ionized metals (seven of 15 sight lines, or roughly 47%; Savage et al. 1993b).

4.2. *Ionization*

Understanding the ionization of the high-velocity gas detected toward Mrk 509 can provide fundamental information on the properties of gas at large distances from the Galactic plane if these clouds are located at large distances from the Sun as suggested by previous studies of H I HVCs in this region of the sky. As an example, Moore & Davis (1994) favor a MS origin involving a hot ($T \sim 10^6$ K) diffuse halo for the Galaxy that exerts a ram-pressure braking of the high-velocity Magellanic Cloud gas after it is stripped by passage through the Galactic disk. In such a scenario, shocks ionize the gas and heat it to high temperatures near the disk, but background radiation from extragalactic sources is the primary ionizing agent for gas at large distances from the plane.

Extended sight lines through the interstellar medium of the Milky Way disk and low halo generally have N(C IV)/N(N V) $\approx 4.6 \pm 2.6$ (Sembach & Savage 1992), and in almost all cases, the absorption from neutral and weakly ionized species is much stronger than that observed for higher ionization states like C IV. The constancy of the high ion ratios along different sight lines has been used to argue for collisional ionization of the gas, and recent models of turbulent mixing of gas (Slavin, Shull, & Begelman 1993) and cooling flows (Shapiro & Benjamin 1993) support this result and predict ionic ratios consistent with those observed for most sight lines. The ion ratios derived for mixed ionization HVCs within a few kiloparsecs of the disk (e.g., HD 156359—Paper II; HD 203664—Sembach 1995) support this result, and in the one definitive case where high-ionization lines are seen at velocities with little or no low ion absorption (e.g., HD 167756—Savage, Sembach, & Cardelli 1994), the ionization properties of the gas are also consistent with an origin in hot, collisionally ionized regions of the interstellar medium.

The high-velocity C IV absorption we detect toward Mrk 509 is unlike any we have previously observed along other sight lines through the Galaxy, except possibly for the C IV HVC at ≈ -215 km s^{-1} toward H1821+643 (Paper IV). The combination of large C IV/N V *and* C IV/Si II ratios argues strongly against a common origin with most of the collisionally ionized gas previously detected in the interstellar medium of the disk or low halo. In Table 3 we provide a comparison of the observed C IV/Si II and C IV/N V ratios in high-velocity gas along sight lines through the Galactic halo studied in previous papers in this series, and it is readily apparent that the ionic ratios are different for this sight line than for most of the others. The C IV/Si II and C IV/N V ratios are less than the lower limits for the two C IV HVC absorption components toward Mrk 509 in all but one case (and even this agreement is marginal since the H1821+643 C IV HVC is very weak). For the C IV/Si II ratio differences in the high-velocity gas clouds to be due solely to carbon and silicon abundance variations requires intrinsic C/Si ratios for the Mrk 509 C IV HVCs that are about an order of magnitude larger than for the other HVCs along the three extragalactic sight lines in Table 3.

In previous papers in this series we have suggested that extragalactic background radiation is a possible source of the ionization of high-velocity gas in the MS toward Fairall 9 (Paper III) and at large Galactocentric radii in the outer warp of the Milky Way (Paper IV), but in both cases it was not possible to rule out other competing ionization processes. Of the possible collisional ionization models that predict substantial amounts of highly ionized gas, only the turbulent mixing layer (TML) models discussed by Slavin et al. (1993) yield large enough C IV/N V ratios to describe the relative quantities of C IV and N V in the C IV HVCs toward Mrk 509. The TML models are particularly successful at producing high C IV/N V ratios because the turbulent mixing causes cooling to set in at low enough temperatures to inhibit the production of the higher ionization states common in most other collisional ionization models (see Sembach & Savage 1992 for a summary of the ionic ratios predicted for other hot gas models). The TML models generally predict N(C IV)/N(N V) $\approx$ 9–20, which is in agreement with the observations, but a collisional ionization interpretation of the C IV HVC absorption toward Mrk 509 suffers from two serious drawbacks. First, the number of TMLs of the type described by Slavin et al. required to reproduce the observed value of log N(C IV) > 14.11 is large ($\geq$45). Second, TMLs are generally associated with significant amounts of neutral and singly ionized gas species contained within the layers as they are initially mixed or as they cool rapidly by line radiation after mixing. We therefore favor photoionization within a warm ($T \sim 10^4$ K) gas as the source of ionization of the C IV HVCs toward Mrk 509.

We have run several photoionization models using the CLOUDY photoionization code (Ferland 1991) with an active galactic nucleus (AGN) power-law photon energy distribution having J_ν(Lyman-limit) $\sim 10^{-22}$ ergs cm^{-2} s^{-1} Hz^{-1} sr^{-1} (see Paper IV and references therein). In Figure 3 we plot the resulting Si II, C IV, and N V column densities as a function of ionization parameter, log Γ ($\equiv n_\gamma/n_H$), and total gas density n_{tot}, for plane-parallel slab models having log N(H I) = 17.0 with $(Z/H)/(Z/H)_\odot \approx 0.2$ (*solid lines and filled symbols*) and log N(H I) = 17.5 with $(Z/H)/(Z/H)_\odot \approx 0.06$ (*dashed lines and open symbols*). Between log $\Gamma \approx -3.0$ and -2.5 the metallicities used for both models represent upper limits imposed by the observed value of log N(Si II) $\leq$ 13.3 in the C IV HVCs. Table 4 contains a summary of the acceptable model results for both of the HVCs *assuming these metallicities*. Note that the range of allowed metallicities encompasses those recently found for MS gas (Paper III) and for the H I HVC toward NGC 3783 (Paper I). In general, log $\Gamma \approx -3.2$ to $\sim$2.6 and log $n_{tot} \approx -2.8$ to -2.2 satisfy the observed constraints listed in Table 1, but lowering the metallicities or neutral hydrogen column densities below the values assumed for these calculations allows for larger ionization parameters and smaller gas density estimates. Of course, geometry, local ionization conditions, and intensity of the extragalactic background will affect these results, but it is probably safe to assume that the C IV HVCs are large ($D \sim$ 1–10 kpc), very diffuse ($\sim 10^{-2}$–10^{-3} cm^{-3}) almost fully ionized [N(H I)/N(H$_{tot}$) < 1%], and of subsolar metallicity. Intermediate-resolution observations of Si III and Si IV toward Mrk 509 would place further constraints on the range of acceptable parameters in the proposed photoionization model and would help to determine the relative importance of collisional ionization and photoionization in the C IV HVCs.

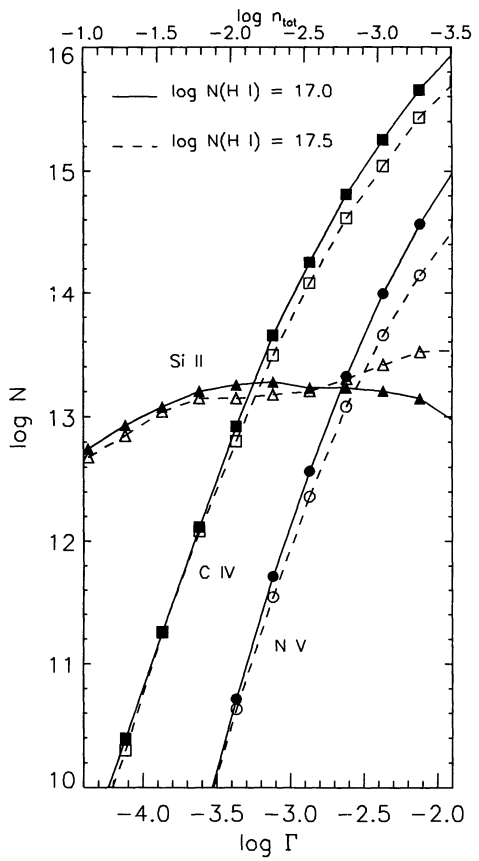

FIG. 3.—Column density vs. ionization parameter for Si II, C IV, and N V produced by an assumed extragalactic radiation field of intensity J_ν(Lyman limit) $\sim 10^{-22}$ ergs cm^{-2} s^{-1} Hz^{-1} sr^{-1} impinging on a plane-parallel gas slab as described in the text. Two models are shown, one for log N(H I) = 17.0 and one for log N(H I) = 17.5. Total gas density is indicated at the top of the figure. The allowable ranges of log Γ and log n_{tot} for the models are listed in Table 4.

TABLE 4

PHOTOIONIZATION MODEL RESULTS

Parameter	log N(H I) = 17.0 $(Z/H)/(Z/H)_\odot \approx 0.2$	log N(H I) = 17.5 $(Z/H)/(Z/H)_\odot \approx 0.06$
	−283 km s^{-1} Component	
log Γ	[−3.0, −2.7]	[−2.9, −2.6]
log n_{tot}	[−2.4, −2.7]	[−2.5, −2.8]
D(kpc)[a]	[2.1, 8.4]	[9.4, 48]
N(H$_{tot}$)/N(H I)	[230, 490]	[610, 1410]
	−228 km s^{-1} Component	
log Γ	[−3.2, −2.7]	[−3.2, −2.7]
log n_{tot}	[−2.2, −2.6]	[−2.2, −2.7]
D(kpc)[a]	[0.8, 5.7]	[2.4, 28]
N(H$_{tot}$)/N(H I)	[140, 380]	[290, 1080]

NOTES.—Values in brackets denote the range of values satisfying the observational constraints listed in Table 1. Note that the range of values for each quantity will change if the metallicity is lower than assumed (see text). The adopted metallicities are upper limits set by the measured Si II column density limit for each HVC component.

[a] D(kpc) is the thickness of the slab used in the model.

4.3. *Relevance to QSO Absorption Line Systems*

The C IV/Si II equivalent width ratios in the Galactic C IV HVCs toward Mrk 509, $W_\lambda(1548)/W_\lambda(1526) > 5.1$ and 1.3, are more typical of the narrow-line heavy-element quasar absorption systems than they are of low-velocity Milky Way disk and halo gas. For example, in the sample of QSO systems observed by Steidel & Sargent (1992), $W_\lambda(1548)/W_\lambda(1526) > 1.1$ (and in many cases greater than 3), whereas in the low-velocity absorption toward Mrk 509, $W_\lambda(1548)/W_\lambda(1526) \approx 0.7$. The equivalent widths of the high-velocity C IV lines are comparable to those estimated for many of the absorption systems in the $0.2 \leq z \leq 2.2$ redshift range of the Steidel & Sargent sample, which means that the high-velocity C IV would produce a typical extragalactic absorption signature of a high-ionization system if viewed from an external vantage point. Note that observations of Mg II or C II toward Mrk 509 are necessary to determine unambiguously whether the C IV HVCs resemble mixed ionization systems because Si II is not always detectable in such absorbers. However, the low H I column density toward Mrk 509 at the velocities of the C IV HVCs encourages comparisons with the higher ionization systems.

The relationship between the ionization properties of QSO metal line systems and those of the Milky Way halo is a subject of debate (see, e.g., Wolfe 1983; Hartquist & Dyson 1984), but the possibility exists that we are only now beginning to explore the outer regions of the Milky Way halo in sufficient detail for comparison with the outer regions of galaxies probed along QSO sight lines. Photoionization of clouds in the extended halos of high-redshift galaxies by extragalactic radiation is widely believed to be responsible for the high-ionization quasar absorption systems (Sargent et al. 1979; Steidel 1990), and given the results of the ionization models discussed in

§ 4.2, the fact that we detect Galactic C IV HVCs toward Mrk 509 with properties closely resembling those of the high-ionization quasar absorption line systems suggests that photons are a viable ionization source for portions of the outer Milky Way as well.

We thank the *HST* and GHRS projects for making these observations possible and Jennifer Sandoval for her assistance with the data handling. We appreciate useful comments from Chuck Steidel. Support for this work was provided through NASA grants HF1038.01-92A (K. R. S.), GO-5300.01-94A (B. D. S.), and HF1062.01-94A (L. L.) from the Space Telescope Science Institute, which is operated by the Association of Universities for Research in Astronomy, Inc., under NASA contract NAS5-26555. E. M. M. acknowledges support from the National Radio Astronomy Observatory, which is operated by Associated Universities, Inc., under a cooperative agreement with the National Science Foundation.

REFERENCES

Bergeron, J., & Boisse, P. 1991, A&A, 243, 344
Blades, J. C., & Morton, D. C. 1983, MNRAS, 204, 317
Bowen, D. V., & Blades, J. C. 1993, ApJ, 403, L55
Bruhweiler, F. C., Boggess, A., Norman, D. J., Grady, C. A., Urry, M., & Kondo, Y. 1993, ApJ, 409, 199
Clemens, D. P. 1985, ApJ, 295, 422
Cohen, R. J., & Mirabel, I. F. 1978, MNRAS, 182, 395
de Boer, K. S., et al. 1994, A&A, 286, 295
Dufton, P. L., Hibbert, A., Kingston, A. E., & Tully, J. A. 1983, MNRAS, 202, 145
Duncan, D. K. 1992, Goddard High-Resolution Spectrograph Instrument Handbook, Version 3.0 (Baltimore: STScI)
Ferland, G. J. 1991, Ohio State Univ. Internal Rep. 91-01
Fitzpatrick, E. L., & Savage, B. D. 1983, ApJ, 267, 93
Foltz, C. B., Chaffee, F. H., Weymann, R. J., & Anderson, S. F. 1988, in QSO Absorption Lines: Probing the Universe, ed. J. C. Blades, D. Turnshek, & C. A. Norman (Baltimore: STScI), 53
Giovanelli, R. 1981, AJ, 86, 1468
Hartquist, T. W., & Dyson, J. E. 1984, ApJ, 279, L35
Hulsbosch, A. N. M., & Wakker, B. P. 1988, A&AS, 75, 191
Lu, L., Savage, B. D., & Sembach, K. R. 1994a, ApJ, 426, 563 (Paper I)
———. 1994b, ApJ, 437, L119 (Paper III)
Mirabel, I. F. 1981, ApJ, 247, 97
———. 1982, ApJ, 256, 112
Mirabel, I. F., & Cohen, R. J. 1979, MNRAS, 188, 219
Moore, B., & Davis, M. 1994, MNRAS, 270, 209
Morton, D. C. 1991, ApJS, 77, 119
Morton, D. C., & Blades, J. C. 1986, MNRAS, 220, 927
Murphy, E., Lockman, F. J., & Savage, B. D. 1995, ApJ, 447, 642
Phillips, M. M., Baldwin, J. A., Atwood, B., & Carswell, R. F. 1983, ApJ, 274, 558
Sargent, W. L. W., Young, P. J., Bocksenberg, A., Carswell, R. F., & Whelan, J. A. J. 1979, ApJ, 230, 49
Savage, B. D., & de Boer, K. S. 1981, ApJ, 243, 460
Savage, B. D., Jenkins, E. B., Joseph, C., & de Boer, K. S. 1989, ApJ, 345, 393
Savage, B. D., et al. 1993a, ApJ, 413, 116
Savage, B. D., Lu, L., Weymann, R., Morris, S., & Gilliland, R. 1993b, ApJ, 404, 124
Savage, B. D., & Sembach, K. R. 1991, ApJ, 379, 345
Savage, B. D., Sembach, K. R., & Cardelli, J. A. 1994, ApJ, 420, 183
Savage, B. D., Sembach, K. R., & Lu, L. 1995, ApJ, in press (Paper IV)
Sembach, K. R. 1995, ApJ, in press
Sembach, K. R., Danks, A. C., & Savage, B. D. 1993, A&AS, 100, 107
Sembach, K. R., & Savage, B. D. 1992, ApJS, 83, 147
Sembach, K. R., Savage, B. D., & Lu, L. 1995, ApJ, 439, 672 (Paper II)
Shapiro, P. R., & Benjamin, R. A. 1993, in Star Forming Galaxies and Their Interstellar Media, ed. J. J. Franco (New York: Cambridge Univ. Press), 273
Slavin, J. D., Shull, J. M., & Begelman, M. C. 1993, ApJ, 407, 83
Spitzer, L., Jr., & Fitzpatrick, E. 1993, ApJ, 409, 299
Steidel, C. C. 1990, ApJS, 74, 37
———. 1993, in Proc. 3d Teton Summer Astrophys. Conf., The Evolution of Galaxies and Their Environment, ed. J. M. Shull & H. A. Thronson (Dordrecht: Kluwer), 263
Steidel, C. C., & Sargent, W. L. 1992, ApJS, 80, 1
Wakker, B. P., & van Woerden, H. 1991, A&A, 250, 509
Wolfe, A. M. 1983, ApJ, 268, L1
York, D. G., Blades, J. C., Cowie, L. L., Morton, D. C., Songaila, A., & Wu, C. C. 1982, ApJ, 255, 467
York, D. G., Ratcliff, S., Blades, J. C., Cowie, L. L., & Morton, D. C. 1984, ApJ, 276, 92